An Upper Ediacaran Glacial Period in Cadomia: the Granville tillite (Armorican Massif) – sedimentology, geochronology and provenance

Ulf Linnemann[1] , Mandy Hofmann[1], Andreas Gärtner[1], Jessica Gärtner[1], Johannes Zieger[1], Rita Krause[1], Robert Haenel[1], Katja Mende[1], Maria Ovtcharova[2], Urs Schaltegger[2] and Pat Vickers-Rich[3,4]

[1]Senckenberg Naturhistorische Sammlungen Dresden, GeoPlasmaLab, Zur Wetterwarte 9, Dresden, 01109, Germany; [2]Department of Earth Sciences, University of Geneva, rue des Maraichers 13, 1205, Genève, Switzerland; [3]School of Earth, Atmosphere and Environment, Monash University, Melbourne (Clayton), Victoria, 3800, Australia and [4]Swinburne University of Technology, Melbourne (Hawthorn), Victoria, 3122, Australia

Abstract

In the Cadomian orogenic belt a package of glacigenic sedimentary deposits have been recently described in the Armorican Massif (Normandy, France). The Granville Tillite Member, the middle part of the upper Granville Formation, is late Ediacaran in age. Maximum depositional ages of the pre- and syn-glacial sedimentary deposits obtained by LA-ICP-MS U–Pb detrital zircon dating indicate a maximum age of 561 ± 3 Ma. Combined with geochronological data on the previously described glacial deposits in Cadomia, West Africa, Arabia and Iran, the Granville Tillite Member appears to represent an Upper Ediacaran Glacial Period in northern peri-Gondwana, clearly younger than the *c.* 580 Ma old Gaskiers glaciation. Detailed mapping and analysis of the depositional regime of two sections near the city of Granville are indicative of two independent glaciomarine lower and upper tillite deposits separated by a distinct conglomeratic marker horizon, evidently a massive gravel beach horizon deposited during an interglacial stage. Age spectra of detrital zircon U–Pb ages constrain the palaeogeographical position of the upper Granville Formation to the periphery of the West African Craton. Post-Gaskiers aged glaciations in Cadomia and in West Africa should be grouped into an Upper Ediacaran Glacial Period dated at *c.* 565 Ma. This glacial period seems not to be related to the negative $\delta^{13}C$ Shuram–Wonoka anomaly. Sedimentary deposits formed during the Upper Ediacaran Glacial Period show a scattered distribution along the marginal orogens of the Gondwana supercontinent independent of palaeolatitude and are coupled most likely to contemporaneous orogenic processes and uplift.

CAMBRIDGE
UNIVERSITY PRESS

1. Introduction

Glaciations have had major impacts on the evolution of life on planet Earth (Hoffmann *et al.* 2004, 2017). Neoproterozoic glaciations most certainly played a major role as a bottleneck for the rise of the Ediacaran biota (Narbonne & Gehling, 2003). Cryogenian (*c.* 850–635 Ma) strata record the most extreme climate episodes in Earth's history. The widespread occurrence of low-latitude glacial deposits fundamentally led to the hypothesis of Snowball Earth (Kirschvink, 1992; Hoffman *et al.* 1998; Kirschvink *et al.* 2000). The Marinoan-aged Snowball Earth (Hoffman *et al.* 1998) has been bracketed between *c.* 635 Ma and *c.* 639 Ma (Hoffmann *et al.* 2004, 2017; Prave *et al.* 2016). Cryogenian global glacial events were followed by the Ediacaran Gaskiers glaciation recognized in Newfoundland, with age constraints of 581–579 Ma (Pu *et al.* 2016). Equivalents with similar isotope age constraints have been described from New England (Thompson *et al.* 2014) and Baltica (Bingen *et al.* 2005). The timing of the Gaskiers glaciation might be used to divide the Ediacaran period into Lower and Upper Ediacaran (Xiao *et al.* 2016). The most significant difference between life before and after this glacial event is the absence of most of the iconic Ediacara biota below and their massive rise and radiation after the Gaskiers glaciation (Narbonne *et al.* 2014; Xiao & Narbonne, 2020). There is no evidence for a global Gaskiers ice age at *c.* 581–579 Ma, as its record is limited to the West Avalonian part of the Appalachians (Youbi *et al.* 2020). However, there is strong evidence that a younger glacial period occurred during late Ediacaran time (560–570 Ma). Geological traces of this event are known from several places in West Africa (e.g. Vernhet *et al.* 2012) and the Cadomian orogenic belt in peri-Gondwanan Europe (Linnemann *et al.* 2018). A compiled dataset points to at least 14 occurrences of Ediacaran glacial deposits worldwide (Youbi *et al.* 2020), which range in age from *c.* 630 Ma to 560 Ma. In this study, all Ediacaran glacial deposits younger than the Gaskiers and Rocky Harbour formations (*c.* 581–579 Ma; Pu *et al.* 2016) are referred

to as the Upper Ediacaran Glacial Period, which had a strong impact on the biota 30 to 20 Ma prior to the onset of the Cambrian period, currently dated at 538.8 Ma (Linnemann *et al.* 2019).

Here, we present new sedimentological and geochronological data from the diamictite-bearing sedimentary succession of the upper Ediacaran Granville Formation in the Armorican Massif (Cadomian orogenic belt of peri-Gondwanan Europe, France; Fig. 1). Such sedimentary units are part of the upper Granville Formation and are characterized by uniquely glaciomarine features. Their maximum depositional ages are provided by laser ablation inductively coupled plasma mass spectrometer (LA-ICP-MS) U–Pb concordia ages of the youngest detrital zircon populations from these clastic sedimentary rocks. In addition, U–Pb LA-ICP-MS detrital zircon ages were used as provenance indicators. Recognition of the glacigenic nature of the Granville Formation is not new, being first suggested by Wegmann (1951) and Wegmann *et al.* (1950), and later by Graindor (1957, 1965) and Doré (1981). This idea was rejected by Eyles (1990), who countered that the Granville tillite was instead a mass flow deposit. A detailed analysis by Letsch *et al.* (2018*b*) pointed out that there was a significantly increased interest in turbidity currents and mass flow processes in the second half of the twentieth century. This change of paradigms led sedimentologists to question the glacigenic nature of many potential tillites, which resulted in a hyper-scepticism of just what diamictites represent. Accordingly, many researchers suggested that diamictites are a product of debris flows (e.g. Schermerhorn, 1974) rather than being related to glaciations. Despite the rejection of the glacigenic nature of the 'Granville tillite' by Eyles (1990), several authors listed it as 'true tillite' without any field description and discussion in view of the existing controversy (e.g. Youbi *et al.* 2020). In this paper, we prefer an alternative assessment and present new data that offer in-depth support for the glaciomarine nature of larger parts of the upper Granville Formation, which crops out in the region around the city of Granville (Normandy, Armorican Massif). Maximum depositional ages of detrital zircons in this formation allow us to constrain the succession to late Ediacaran and post-Gaskiers time. Further, we discuss how the sediments of the Granville Tillite Member of the upper Granville Formation record the occurrence of an Upper Ediacaran Glacial Period and its relationship to the strong negative δ^{13}C excursion of the Shuram–Wonoka anomaly. A correlation to related glaciations in Cadomia and adjoining areas helps to improve our understanding about the nature of the Upper Ediacaran Glacial Period.

2. Geological framework

The Cadomian orogenic belt forms a superterrane along the northern periphery of the West African continent that was active in late Ediacaran time (Fernandez-Suarez *et al.* 2000; Linnemann *et al.* 2000, 2004, 2014; Nance *et al.* 2010). The most prominent outcrops of this superterrane occur in modern peri-Gondwanan Europe (Iberia, France, Bohemia, basement of the Pyrenees and Alps; Fig. 1). The so-called 'Cadomian basement' is made up of volcano-sedimentary successions and plutonic rocks ranging in age from *c.* 580 Ma to 537 Ma (Linnemann *et al.* 2014). The overall setting is interpreted to be a geotectonic assemblage of magmatic arcs and back-arc basins (Linnemann, 2007). A recent plate tectonic analogue of this Ediacaran-aged sequence is the western Pacific Ocean (Murphy & Nance, 1991). The largest part of the sedimentary record of Cadomia was evidently deposited in a back-arc

setting (Linnemann, 2007; Linnemann *et al.* 2014). Maximum depositional ages of detrital zircons from several locations point to the opening of the Cadomian back-arc basin in a time window of *c.* 570–565 Ma, and final post-deformational Cadomian orogenic processes are characterized by a strong plutonic event at *c.* 540–537 Ma. (e.g. Linnemann *et al.* 2014). Glaciomarine strata in the Cadomia sequence are reported from the Bohemian Massif (Saxo-Thuringian Zone) and Iberia (Central Iberian Zone), which have maximum depositional ages of *c.* 565 Ma (Linnemann *et al.* 2018). Recent field observations and U–Pb zircon data show a strong linkage of Cadomia with coeval Neoproterozoic crustal units in the Anti-Atlas of Morocco (Vernhet *et al.* 2012; Letsch *et al.* 2018*a*; Errami *et al.* 2021).

The classic area of outcrop recording the Cadomian orogeny and emplacement of the Cadomian basement, respectively, is the Armorican Massif in northern France (Bertrand, 1921) (Fig. 1). The first description of an unconformity related to Cadomian orogenic processes was that in Normandy by Bunel (1835), and much later by Graindor (1957). An active margin setting for Cadomian basement rocks, including the entire Armorican Massif, was proposed by various French authors (e.g. Chantraine *et al.* 1994). This Armorican Massif can be subdivided into the major North-Armorican, Central-Armorican and South-Armorican domains (Ballèvre *et al.* 2009). All three domains were formed by the Variscan orogenic processes during Pangaea assembly and show widespread occurrences of an inherited pre-Variscan consolidated Cadomian basement (Ballèvre *et al.* 2009). In addition, there is also an exotic terrane in the Armorican Massif represented by the northwestern situated Léon Domain, which shows a possible relationship to the Mid-German Crystalline Rise (Faure *et al.* 2010).

Our scientific target, the Granville Formation, was previously highlighted by Dupret (1984). The formation is part of the Cadomian basement in the North-Armorican domain and has been described as a low-grade, metamorphosed, late-orogenic succession of siliciclastic rocks. The Granville Formation is tectonically isolated and fault-bound from adjoining tectonostratigraphic units. The presence in the Granville Formation of black chert pebbles constrains the Granville succession to the upper part of the Brioverian Supergroup (Chantraine *et al.* 1994). Wegmann *et al.* (1950, 1951) and Graindor (1957, 1965) suggested a glacigenic origin for the black chert, pebble-bearing strata of the Granville Formation. Eyles (1990), to the contrary, suggested the sedimentary deposits of the Granville Formation were debris flows and 'gravel turbidites' with no glacial influence.

3. Sedimentology and glaciomarine features

To address this issue of origin of the contested sediments, our field investigations focused on the area around the city of Granville (Normandy, Armorican Massif; Figs 1, 2). A steep, rocky coast along the Atlantic Ocean formed by strong tides and heavy storms offers excellent and fresh outcrops of the Granville Formation (Fig. 2). Except for limited and often temporary outcrops (owing to construction in the city area), the greatest part of the Granville Formation crops out along the coast to the west of the city of Granville. Our recent mapping and documentation of several sections in this area has revealed that this formation can be subdivided on an informal level into a lower and an upper part, here named as the lower and upper Granville formations (Fig. 2). The lower Granville Formation primarily is composed of a dark greenish-grey, immature, massive and thick-bedded quartzite, best exposed
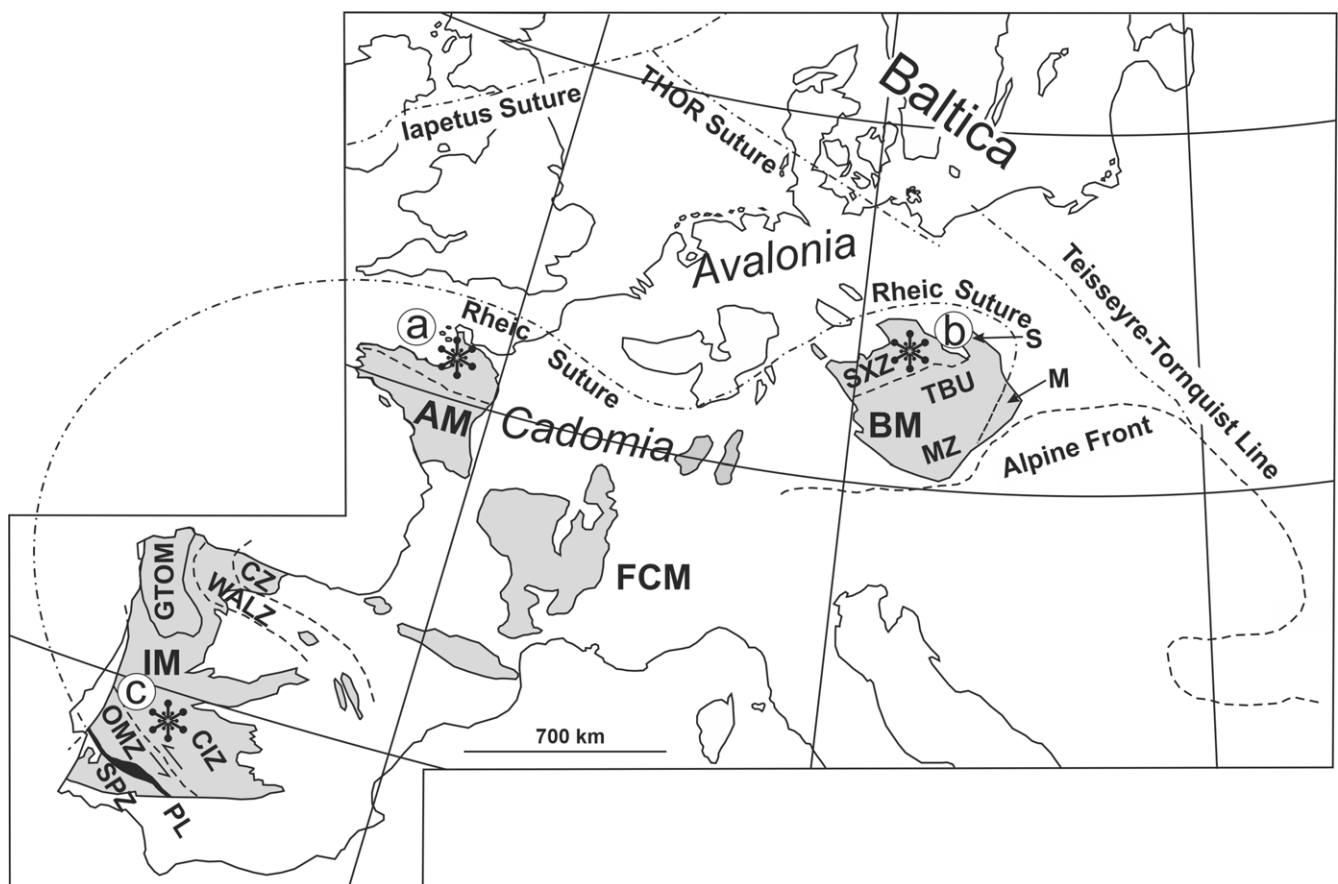
Fig. 1. Location of glaciomarine deposits in the Cadomian basement of Central and Western Europe: AM – Armorican Massif; BM – Bohemian Massif; FCM – French Massif Central; IM – Iberian Massif; M – Moravo-Silesian unit; S – Sudetes. Variscan zones: CIZ – Central Iberian; CZ – Cantabrian; GTOM – Galicia-Tras os Montes; MZ – Moldanubian; OMZ – Ossa Morena; PL – Pulo do Lobo; SPZ – South Portuguese; SXZ – Saxo-Thuringian; TBU – Teplá-Barrandian unit; WALZ – West Asturian–Leonese. Upper Ediacaran glaciomarine deposits in the Cadomian orogen: a – Granville (Armorican Massif); b – Weesenstein and Clanzschwitz (Bohemian Massif); c – Orellana (Iberian Massif) (modified from Linnemann *et al.* 2018).

along the coast west of the Musée Christian Dior and north of the Rue de la Plage (Fig. 2). The best exposed outcrops of the upper Granville Formation occur at Cap Lihou and Pointe du Lude (Fig. 2). The entire formation has a general NE–SW-directed strike and dips between 30 and 45 degrees towards the NW (Fig. 2). Likely glacigenic deposits occur in the upper Granville Formation, which is composed of a diverse siliciclastic sedimentary sequence including mudstones, quartzites, diamictites, conglomerates and sandy turbidites. For this study our team mapped and sampled in detail the lithologies in the upper Granville Formation at two locales: section 1 at the Rue de Cap Lihou and section 2 at Pointe du Lude (Fig. 2). Both sections can be linked to each other using a marker horizon consisting of a prominent conglomerate (Figs 2, 3). This is the only conglomerate bed in the formation and thus a unique tool for correlation and reconstruction of the depositional setting (Figs 3, 4).

Owing to limited exposure, the contact between the lower and upper Granville formations is not exposed in section 1. On an informal level, the upper Granville Formation is subdivided into three members with several units based on its diverse lithological composition (Fig. 3). Unit 1A of the section is ~48 m thick and predominantly composed of mudstones alternating with thin- and thick-bedded quartzites (Fig. 3). This unit is interpreted as a pre-glacial member 1 of the upper Granville Formation. The overlying 32 m thick unit 1B is a diamictite with a 5.9 m thick layer of platy thin-bedded quartzite in the middle. The diamictite matrix is

composed of greywacke and mudstone. Matrix-supported pebbles embedded in the diamictite include granite, sandstone, chert, quartzite and vein quartz. The size of the well- to sub-rounded pebbles ranges from several millimetres up to 6 cm. Some of these pebbles are associated with typical impact marks normally associated with diamictites, having a glaciomarine tillite origin. A 2.5 m thick conglomerate horizon (unit 1C) overlies the lowest diamictite of section 1. The conglomerate is component supported, with sub- to well-rounded pebbles averaging 2–5 cm in diameter. The clast composition is similar to that of the underlying diamictite. The overlying units begin with a 4 m thick mudstone containing rare dropstones followed by another 7.5 m thick diamictite with similar features to the lower diamictite in section 1. The uppermost layer of unit 1D is a 2.5 m thick, well-bedded quartzite overtopped by a modern soil (Fig. 3). The conglomerate (unit 1C) lies between the lower and the upper tillites (Fig. 3). Both tillites (units 1B, 1D) and the conglomerate in between make up member 2 of the upper Granville Formation, for which the term Granville Tillite Member is suggested (Fig. 3).

Section 2 crops out at the Pointe du Lude cliffs, offering outstanding exposure at low tide (Figs 3, 4). The northernmost part of the cliff section (Fig. 4) provides the best exposure of members 1–3 of the upper Granville Formation. The outcrops exposed along the western cliff offer excellent exposure of members 1–3 at low tide. Here, at the southernmost part at the coast and directly downhill north from the Musée Christian Dior, the contact between the
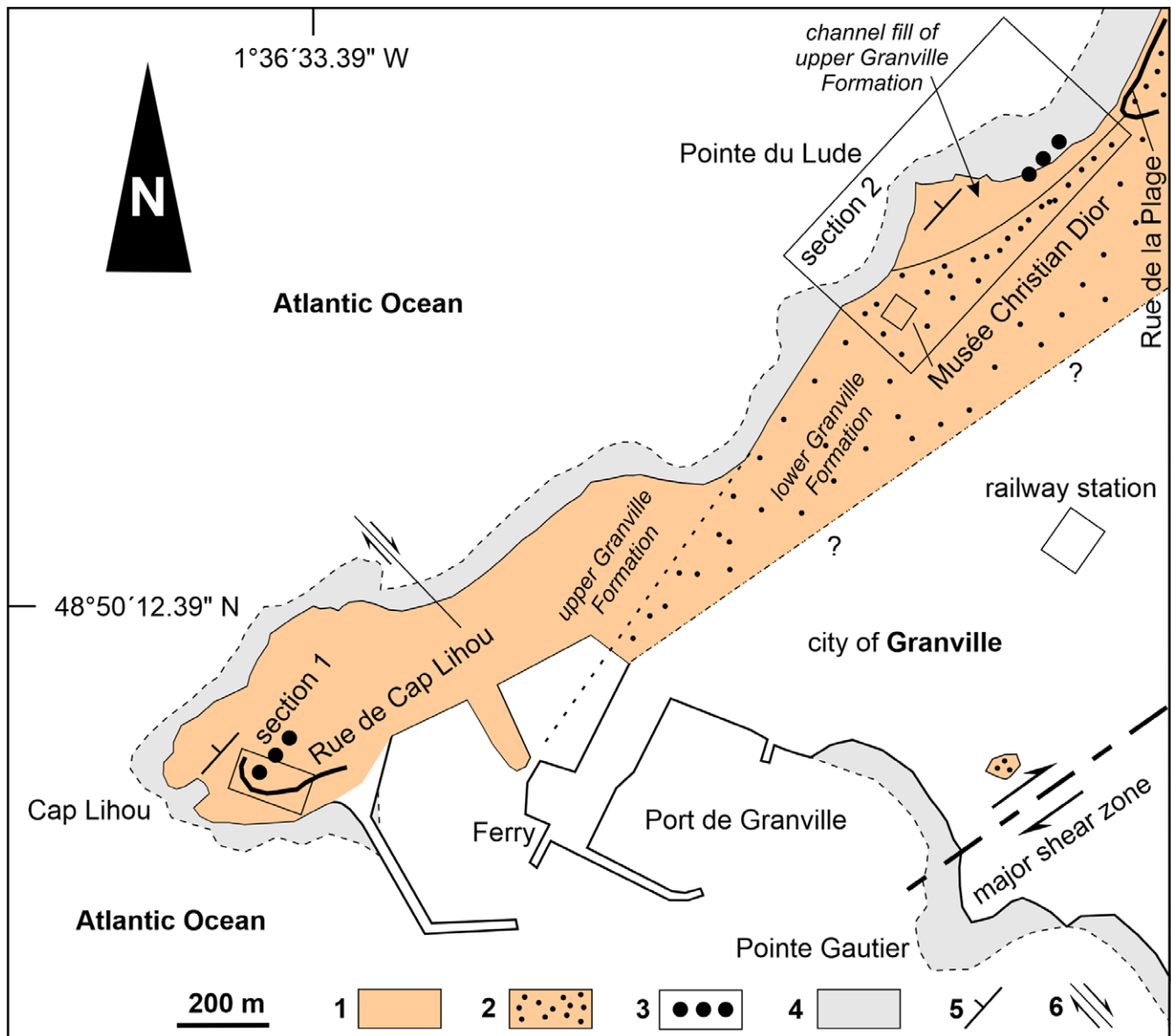
Fig. 2. Geological map from the area of the city of Granville (Armorican Massif) showing the distribution of the Granville Formation, the location of documented sections and the position of a marker horizon. 1 – upper Granville Formation; 2 – lower Granville Formation; 3 – marker horizon (conglomerate); 4 – beach and outcrops exposed at low tide; 5 – strike and dip; 6 – strike-slip fault.

lower and upper Granville formations (Fig. 4) is exposed. Section 1 differs in its lower part from section 2. It begins at beach level immediately south of the switchback of the Rue de la Douane with mudstones where, in contrast, such a contact with the underlying lower Granville Formation is not exposed in the northern cliff (Fig. 4). The mudstones in this lower unit 2A are ~15 m thick (Figs 3, 4) and consist of extremely thin-bedded, fine-grained turbidites (Fig. 5a) partly exhibiting a rhythmic arrangement (Fig. 5b), likely reflecting a seasonal and/or process-controlled sedimentation regime. The mudstones appear to be equivalent to member 1 of section 1 (Fig. 3).

The mudstones do not crop out along the western cliff (Fig. 4) and pinch out to the SW. Along the western cliff, unit 2B directly overlies the monotonous, massive, thick-bedded quartzite of the lower Granville Formation (Fig. 4). Units 2B to 2E (Fig. 3) up-section reflect a dramatic reduction in thickness compared to that

present in outcrops of the northern to western part of the cliff (Fig. 4). The map in Figure 4 showcases the spatial arrangement of the sedimentary units interpreted as deposits formed in a glacial valley incised into the massive quartzite of the lower Granville Formation. Such a valley could have been formed by fluvial erosion of the lower Granville Formation prior to glaciation, so reflecting an erosional unconformity between the lower and upper Granville formations. The suggested base of the incised valley and an assumed onlap contact of member 1 are marked in Figure 4.

The 4 m thick unit 2B (Fig. 3) lies above the mudstones (unit 2A) exposed on the northern cliff and above the massive quartzite of the lower Granville Formation exposure along the western cliff. Unit 2B hosts features indicating a strong glacigenic overprint of proglacial sediments, such as fluvial conglomerates and sandstones (Fig. 6). Deformation appears to have occurred during ice–sediment coupling associated with changing porewater pressures
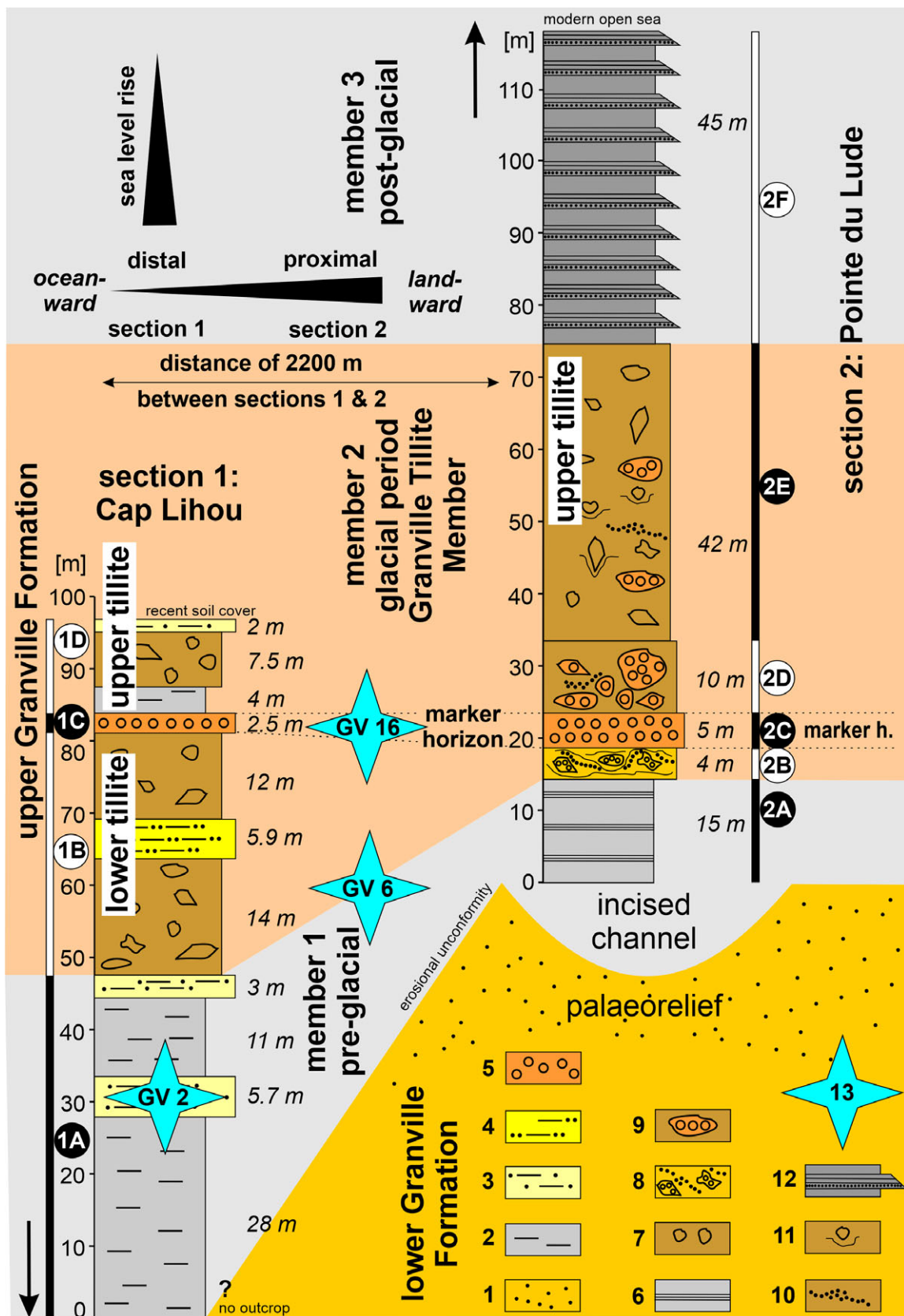
Fig. 3. Lithological columns of two documented sections of the Granville Formation situated at the road-cut in the Rue de Cap Lihou (section 1) and at the cliff at Pointe du Lude (section 2). 1 – massive quartzite of the lower Granville Formation; 2 – mudstone; 3 – intercalation of thin-bedded quartzite and mudstone; 4 – thick-bedded quartzite; 5 – conglomerate (marker horizon); 6 – varve-like very thin-bedded and partial rhythmic arranged turbidites; 7 – diamictite composed of a greywacke-matrix, pebbles up to 6 cm in diameter; 8 – unit of subglacial sediment mingling and ice-coupled glacigenic deformation structures affecting siliciclastic deposits; 9 – fragments of conglomerate (erratic blocks) embedded in a matrix of diamictite; 10 – pockets of sand and fine-grained conglomerate in a matrix of diamictite; 11 – frequent occurrence of dropstones; 12 – sandy turbidites; 13 – sample location.
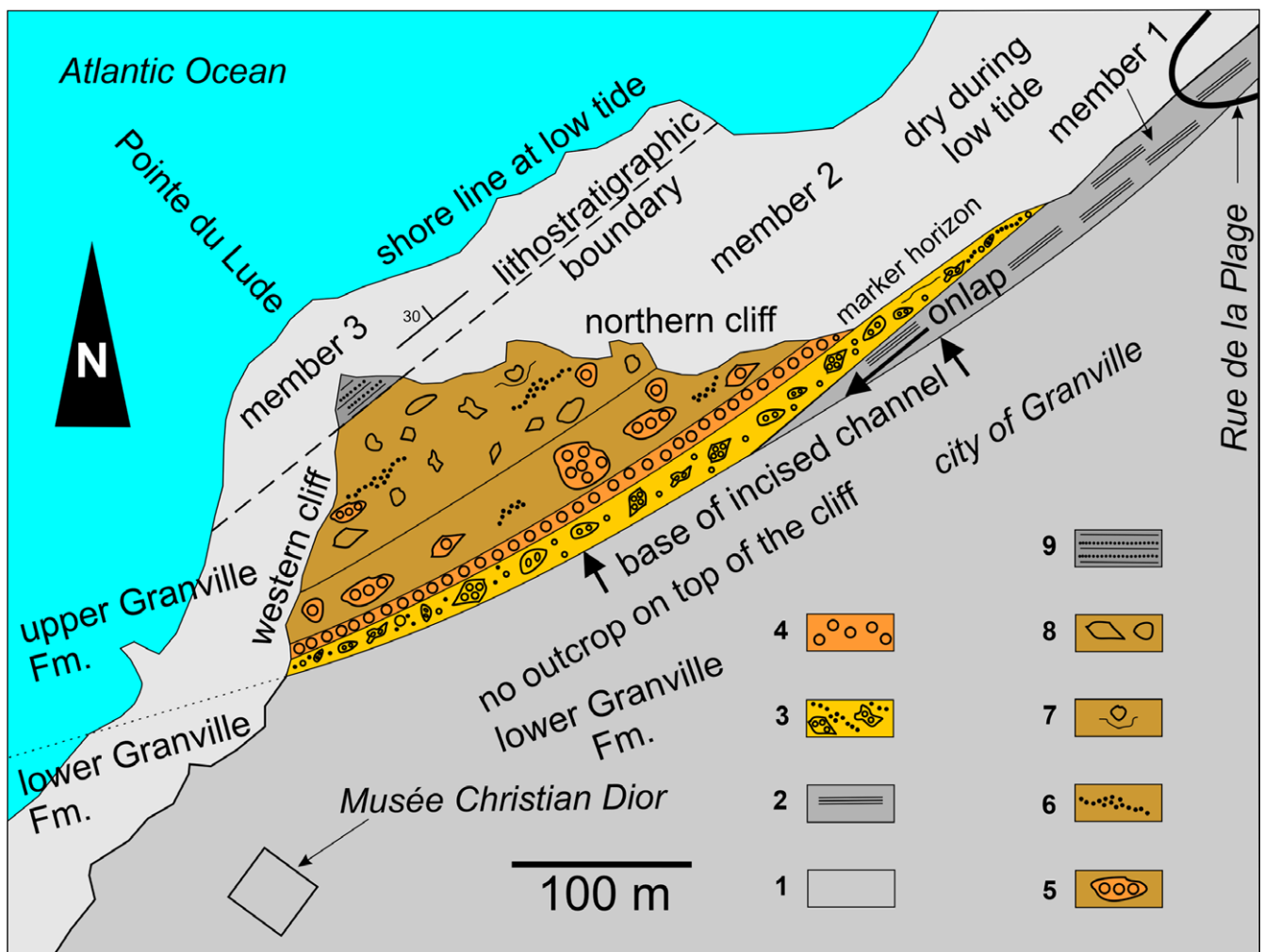
Fig. 4. Detailed geological map of the lower and upper Granville formations of section 2 at Pointe du Lude south of the Rue de la Douane (city of Granville). 1 – massive quartzites of the lower Granville Formation; 2 – varve-like very thin-bedded and partially rhythmic arranged turbidites; 3 – macro-scale glacigenic deformation structures affecting siliciclastic deposits; 4 – conglomerate (marker horizon); 5 – fragments of conglomerate (erratic blocks) embedded in a matrix of diamictite; 6 – pockets of sand and fine-grained conglomerate in a diamictite matrix; 7 – frequent occurring dropstones; 8 – diamictite composed of a greywacke-matrix and pebbles (in part dropstones) up to 6 cm in diameter; 9 – sandy turbidites of member 3 of the upper Granville Formation.

and strain rates. Ring-like arranged turbate structures occur in a mixture of mudstone matrix and fragments of *in situ* brecciated conglomerates (Fig. 6a, b). Furthermore, there are imbricated deformation structures of sandstone penetrating into the conglomerates during soft sediment deformation processes caused by ice–sediment coupling (Fig. 6c, d). Also present are imbricated deformation structures of load-structures formed during such soft sediment deformation processes (Fig. 6d). Such phenomena can be explained by ice-load and flow-directed stress (Fig. 6d). Turbate structures and imbricated deformation structures induced by ice-load and ice–sediment interactions during glacier growth, overstepping proglacial sediments, have been reported over the last decade with respect to fossil occurrences (Ravier *et al.* 2014) and are clearly observable in recent glacial settings (Skolasińska *et al.* 2016). We suggest that unit 2B was formed contemporaneously with the deposition of the lower tillite (unit 1B) exposed in section 1 (see stage 1 in Fig. 8) and formed by the glacial advance below the glacier. Unit 2B appears to have been formed owing to the overriding by the proglacial sediments in a channel (Fig. 8, stage 1). Unit 2B offers insight into the interaction of glacial tectonics and temperature effects. Conglomerate blocks in Unit 2B show shearing ('bookshelf tectonics'). Shear planes

are restricted to the blocks and do not cross-cut the surrounding sedimentary matrix. In the muddy matrix often a schlieren-like arrangement of irregular conglomerate shreds is visible (Fig. 7). Such structures point to an *in situ* fluidization of the conglomerate block resulting in a visible mingling of conglomerate schlieren and mudstone. The situation suggests rip-up and re-embedding of a frozen block of gravel, its ice-coupled deformation in the plastic sediment and final fluidization by marginal melting and mingling with the sedimentary substrate (Fig. 7).

The conglomeratic marker horizon exposed in section 1 (unit 1C) is also present in section 2, represented by a 5 m thick conglomerate (unit 2C; Fig. 3). Sub- to well-rounded pebbles range in size from 1 to 5 cm and are composed predominantly of sedimentary components (quartzites, greywackes, black cherts) and vein quartz (Fig. 5c). Granite pebbles and other types of igneous lithologies are rare. Taking into account the reconstruction of the geological history recorded in both sections prior to the deposition of the conglomeratic marker horizon, we suggest that deposition of this conglomerate occurred after glacial retreat. Thus, we propose that this unique conglomerate, a true marker horizon, was deposited as a massive beach gravel-conglomerate resulting from

Fig. 5. Primary sedimentary structures and features of the Granville Tillite Member (upper Granville Formation) in section 2 (Pointe du Lude). (a) Thin-bedded turbidites of member 1 (upper Granville Formation, unit 2A, length of hammer head = 16 cm). (b) Detailed view on strata shown in (a): very thin-bedded and cyclic arranged turbidites (unit 2A, diameter of coin = 2.3 cm). (c) Conglomerate (marker horizon) containing pebbles of black chert (unit 2C, length of hammer head = 16 cm). (d) Sub-rounded ice-rafted fragment of conglomerate (erratic block) embedded into diamictite (unit 2D, length of hammer = 33 cm). (e) Dropstone of an angular fragment of a granite pebble (unit 2E, diameter of coin = 1.9 cm). (f) Ice-rafted debris and a dropstone of a well-rounded pebble of coarse-grained sandstone (unit 2E, diameter of coin = 2.3 cm). (g) Dropstone of a well-rounded quartzite pebble (unit 2E, diameter of coin = 1.9 cm). (h) Sketch of image shown in (g) that illustrates more clearly the different lithologies, bedding and structures made by the impact of the dropstone.
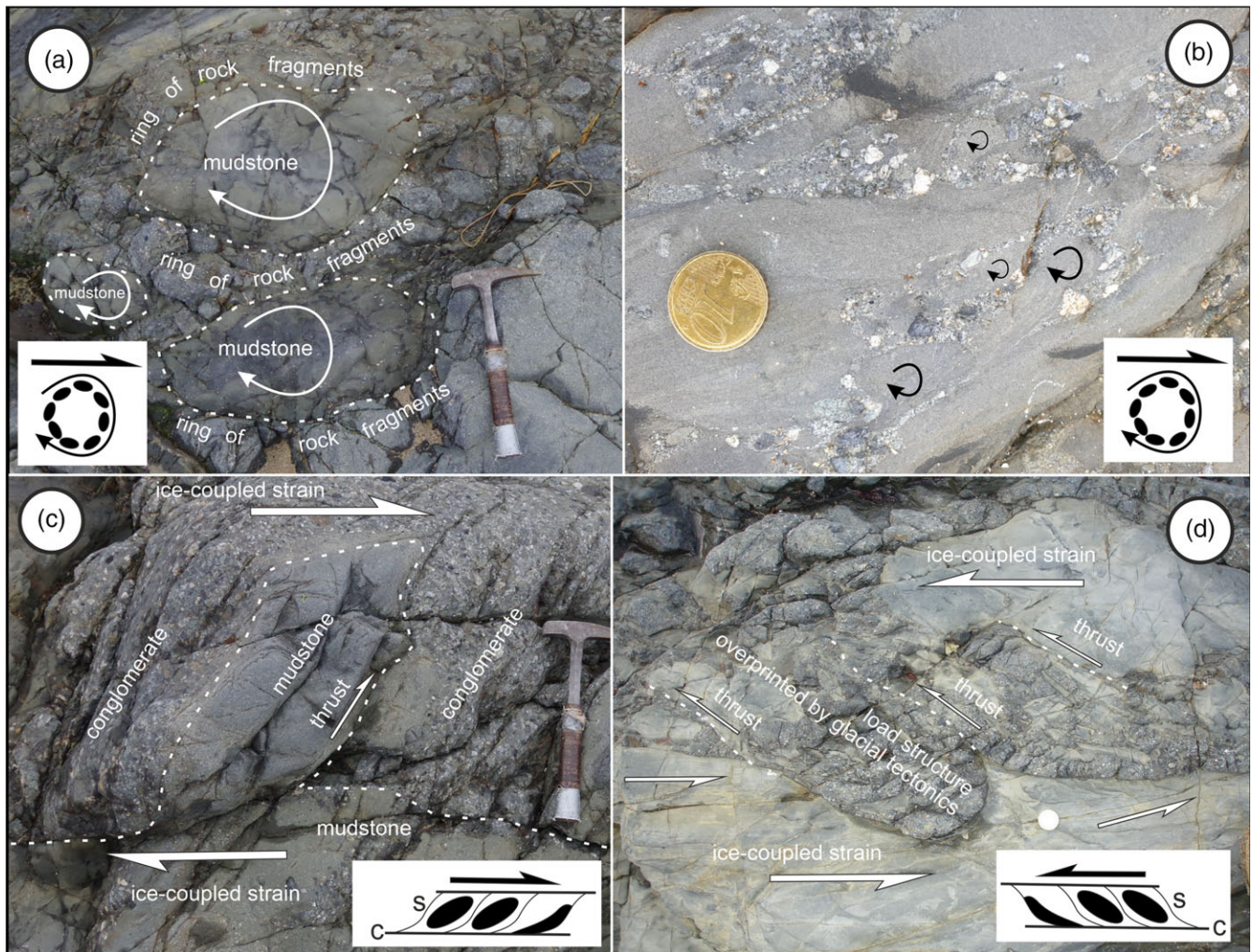
Fig. 6. Glacigenic deformation structures of proglacial sedimentary infill of a glacigenic channel incised into the massive quartzite of the lower Granville Formation. The outcrop is situated at the northern end of the cliffs at Pointe du Lude. Deformation originated during ice–sediment coupling associated with porewater pressures and strain rates. (a) Turbate structures in a mixture of rotated mudstone balls and ring-like arranged fragments of *in situ* brecciated conglomerate (unit 2B, length of hammer = 33 cm). (b) Small turbate structures in a mixture of a mudstone matrix and well- to sub-rounded pebbles (unit 2B, diameter of coin = 1.9 cm). (c) Imbricated deformation structure of mudstone penetrating into a conglomerate during soft sediment deformation processes caused by ice–sediment coupled shearing (unit 2B, length of hammer = 33 cm). (d) Load structure overprinted by micro-thrusts and imbricated deformation under ice-coupled strain. Please note: micro-thrusts do not cut the entire rock because they were formed in a soft sediment prior to lithification (unit 2B, diameter of coin = 2.3 cm).

an interaction of meltwater which produced outwash fans in front of the retreating ice sheet. Likely these fans were reworked then by the surf along the beach. Ongoing sea level rise may have intensified this process (Fig. 8, stage 2). Similar observations of recent settings are known from the coasts along the margins of glaciated areas (Davis & Fitzgerald, 2004).

A second ice advance and ongoing subsidence due to ice and sediment load on the shelf apparently led to the formation of the upper tillite, which occurs in both of the measured sections (Figs 3, 8, stage 3). In section 2, the lower 10 m of the upper tillite (unit 2D; Figs 3, 4) contains large, sub-rounded to angular, up to metre-sized blocks of the underlying conglomerate (Fig. 5d). Such blocks most likely were formed as rip-up clasts from the conglomeratic marker horizon during glacier advance, which were then subsequently transported as boulders in the tillite matrix (Fig. 8, stage 3). Up-section a 42 m thick second tillite occurs (unit 2E, Fig. 3), which contains abundant ice-rafted dropstones underlain by clear impact structures (Fig. 5e–h). Most of the dropstones have sedimentary lithologies (Fig. 5). One exceptional angular fragment

of a granite (Fig. 5e) witnesses fragmentation by stress induced by the glacial ice before the granite became embedded into the tillite as an ice-rafted dropstone. This feature documents the increasing involvement of floating ice and/or icebergs into the sedimentary regime. Unit 2E of the upper tillite also contains rare rip-up clasts of conglomerate fragments and sand pockets, fine-grained conglomerate and pebbles in a diamictite matrix, commonly referred to as ice-rafted debris. Layers made of clasts and sand forming pockets were evidently originally concentrated on the surface of melting icebergs and ice floes and subsequently sank en masse to the sea floor.

The upper tillite in section 2 is overlain by a succession of sandy turbidites, which form unit 2F and the post-glacial member 3 of the upper Granville Formation at Pointe du Lude (Figs 3, 4). One can trace that part of the section for 45 m at low tide before it dips shallowly into the ocean (Fig. 4). The occurrence of post-glacial turbidites above the glacigenic sedimentary rocks suggests a significant deepening of the basin, but this is difficult to explain by sea-level rise caused only by melted ice and subsidence. Thus, we suggest

Fig. 7. Detailed view on a marginal area of a block of a conglomerate embedded in unit 2B (section 2, Pointe du Lude, upper Granville Formation). The conglomerate block shows shearing ('bookshelf tectonics'). Shear planes are restricted to the block and do not cross-cut the sedimentary matrix around the block. In the muddy matrix a schlieren-like arrangement of irregular conglomerate shreds is visible. Length of hammer head is 16 cm.

that an additional deepening was forced by rifting in the Cadomian back-arc basin associated with the establishment of submarine turbidite fans (Fig. 8, stage 4).

4. U–Pb ages and provenance

Unfortunately, no ash beds or any significant fossils are known from the Granville Formation. Thus, dating can only be estimated based on included detrital zircons. Based on three samples of siliciclastic rocks from section 1, detrital zircons from heavy mineral concentrates were extracted and analysed employing U–Pb LA-ICP-MS age dating. Heavy mineral separation and isotopic analyses were carried out at the GeoPlasmaLab of the Senckenberg Collections of Natural History Dresden. The analyses of U–Th–Pb isotopes were performed with a RESOlution 193 nm excimer laser (Applied Spectra) connected with a single-collector ICP-MS ELEMENT 2XR (Thermo Fisher Scientific). More details of the analytical procedure, co-ordinates of sample locations and isotope data are available in the online Supplementary Material. Concordia age plots were generated by making use of Isoplot 4.15 (Ludwig, 2008). Kernel density estimation plots were produced using the *detzrcr* package for the statistical program R 3.6.1. by Anderson *et al.* (2018).

Sample GV2 (platy quartzite) was taken from the pre-glacial member 1 of the upper Granville Formation. Samples GV6 (greywacke, tillite matrix) and GV16 (conglomerate, marker horizon) were collected from member 2 (Granville Tillite Member, section 1). The positions of the samples in the section are shown in Figure 3.

Maximum depositional ages from all three samples were calculated based on the youngest detrital zircon populations and all were in the same range. Concordia ages varied slightly from 561 ± 3 Ma ($n = 11$, GV16) via 562 ± 3 Ma ($n = 12$, GV 2) to 564 ± 8 Ma ($n = 3$, GV6) (Fig. 9). Thus, sedimentary deposits of the upper Granville Formation are younger than *c.* 562 Ma. The upper limit of its depositional age is limited by the massive granitoid plutons in the Mancelian region intruded into the upper Brioverian supergroup at *c.* 550–540 Ma (D'Lemos *et al.* 1990). The age of the glacial period expressed in the tillites of the upper Granville Formation is bracketed in a time period of *c.* 562–540 Ma and falls into the latest Ediacaran. Similar age constraints are known from the two other occurrences of glaciomarine tillites in Cadomia situated in Iberia and Bohemia (Linnemann *et al.* 2014, 2018).

U–Pb ages derived from detrital zircons are useful tools for provenance studies, important for our understanding of patterns of crustal growth in the hinterland. All three samples of clastic sediments from the upper Granville Formation show a very similar distribution pattern of zircon populations (Fig. 10) typical for Cadomia and its West African hinterland (Linnemann *et al.* 2014, 2018). The U–Pb ages of the detrital zircons from this study can be grouped in six major categories (Fig. 10): (i) late Ediacaran zircon ages related to the Cadomian orogeny *sensu stricto* (*c.* 580–560 Ma), (ii) early Ediacaran zircons that have an affinity to pre-Cadomian (Pan-African?) magmatic activity (*c.* 680–580 Ma),
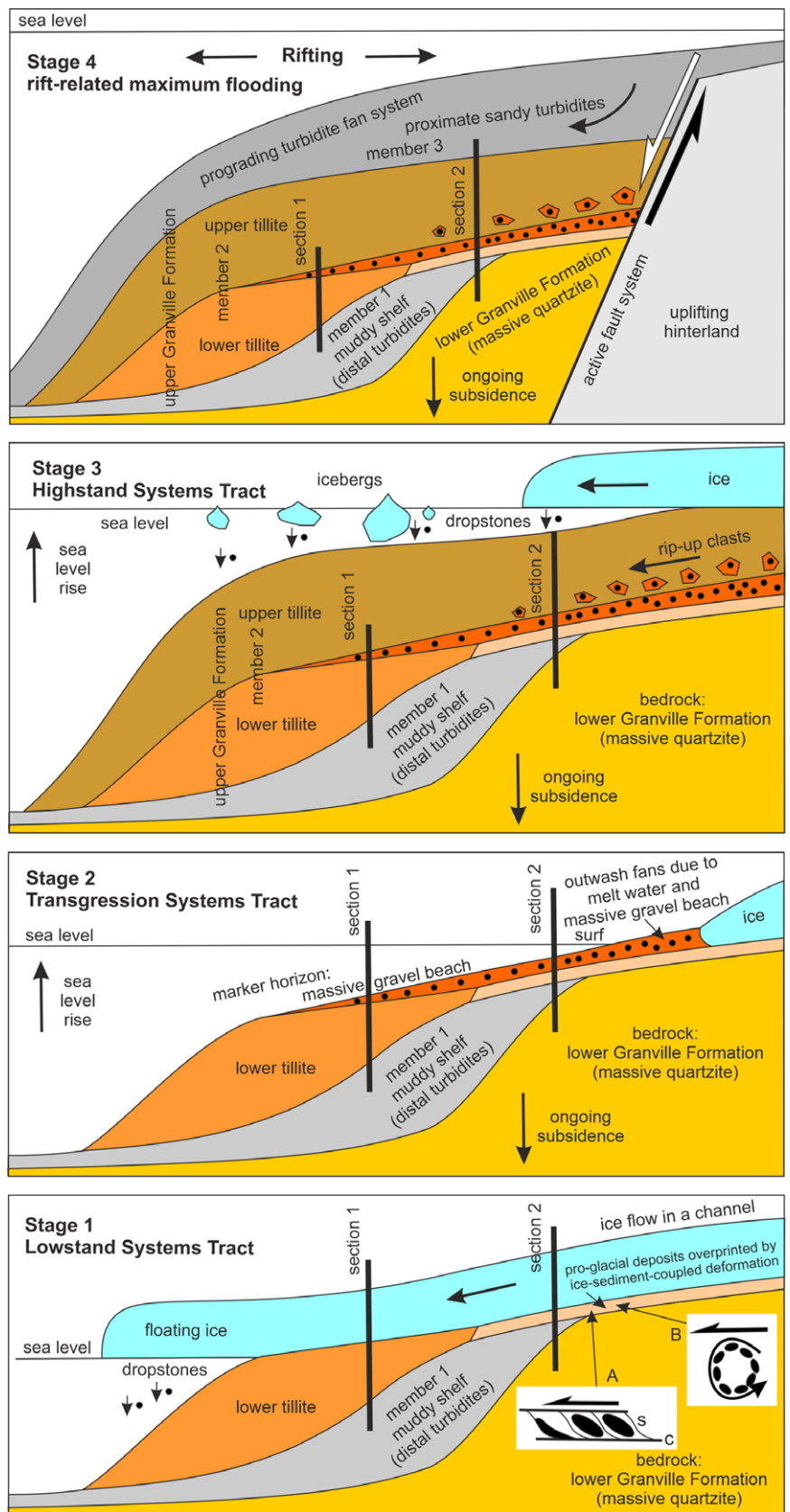
Fig. 8. Model with four stages illustrating the deposition and tectono-sedimentary regime of the lower and upper Granville formations. Positions of sections 1 and 2 are indicated. Deformation of proglacial deposits in a channel incised into the massive quartzite of the lower Granville Formation is indicated by signatures for imbricated deformation (A) and turbate structures (B).
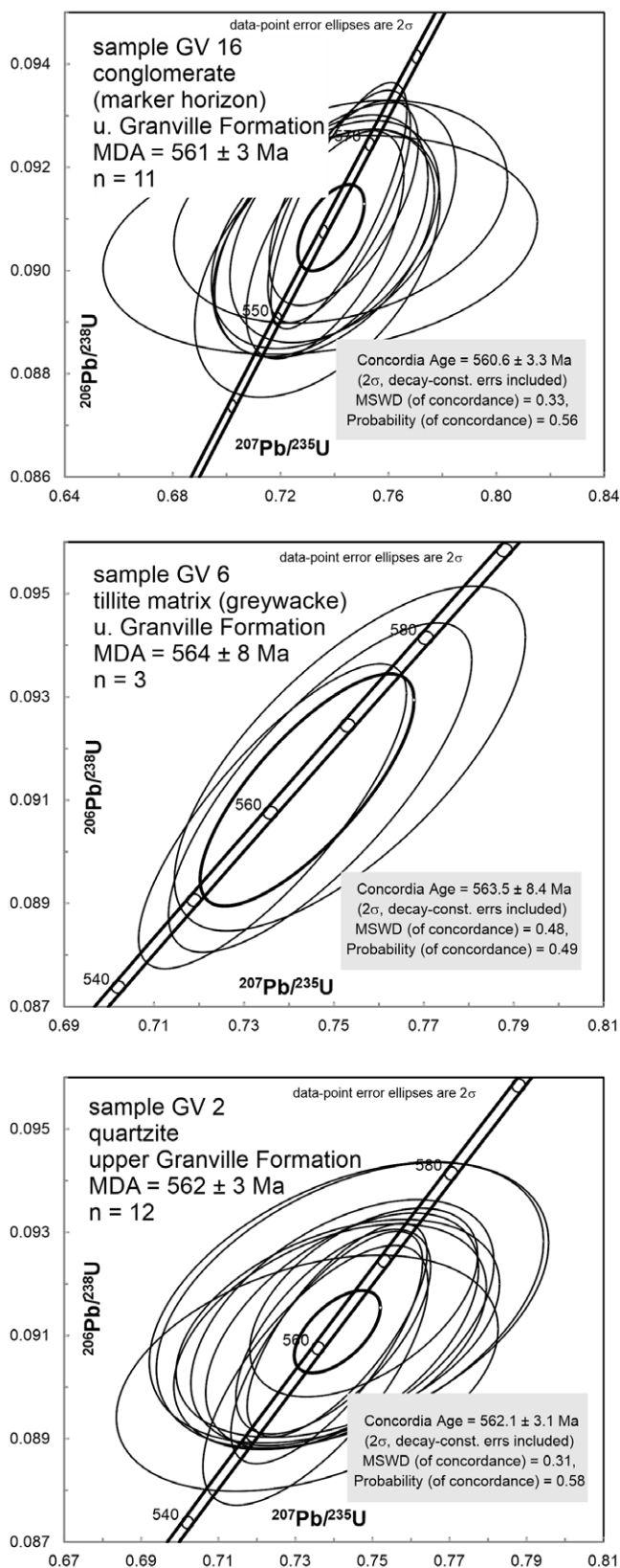
Fig. 9. Maximum depositional ages (MDA) of samples GV2, GV6 and GV16 (lower Granville Formation) derived from U–Pb LA-ICP-MS ages of the youngest detrital zircon populations of each sample.

(iii) zircon grains showing an age range of *c.* 900–680 Ma most probably derived from West African magmatic arcs, dykes and oceanic complexes, (iv) zircons formed during the activity of post-Eburnean arcs and magmatic events (*c.* 1950–900 Ma), (v) zircons related to the Eburnean Orogenic event of the West African Craton (*c.* 2200–1950 Ma) and (vi) pre-Eburnean, mostly Archaean zircon grains related to Liberian and Leonian orogenic events and the old nuclei of the West African Craton (Potrel *et al.* 1998). Exact percentages of these populations are available from Figure 10. The Palaeoproterozoic and Archaean pattern is typical of a West African Craton provenance (e.g. Linnemann *et al.* 2000, 2014; Abati *et al.* 2010, 2012). Neoproterozoic zircon populations are diagnostic of provenance from the Cadomian orogen and from the Pan-African basement of the Trans-Saharan Belt or a related area (Linnemann, 2007; Linnemann *et al.* 2011; Drost *et al.* 2011). The rare Mesoproterozoic zircons might well have been derived from the cratonic neighbours of the West African Craton, which were at *c.* 570–560 Ma the Amazonian or Sub-Saharan Cratons (e.g. Gärtner *et al.* 2013).

5. Discussion and conclusion

Sedimentary features, aspects of basin development, the plate tectonic framework and U–Pb ages, all considered together, allow the reconstruction of Ediacaran glacial processes, palaeogeography and timing of orogenic processes in that part of the Cadomian orogen, which is preserved in the Granville Formation (North-Armorican Domain, Normandy, Armorican Massif). Sedimentary and other features of the deposits further allow tracing a glacial period within sedimentary rocks related to the Cadomian orogen. Indicative of a glaciomarine deposition are ice-rafted dropstones, ice-rafted debris and deformation structures, the direct result of ice-load and ice–sediment interactions associated with changing porewater pressures and strain rates. The latter are represented by turbate structures, *in situ* brecciation and imbricated deformation in a pre- to syn-diagenetic stage.

Pre-glacial, glaciomarine and post-glacial sedimentation took place in a time span of *c.* 562–540 Ma. Age constraints completely rule out a correlation of this Upper Ediacaran Glacial Period recorded in the upper Granville Formation with the Gaskiers glaciation, which occurred at *c.* 581–579 Ma (Bowring *et al.* 2002; Thompson *et al.* 2014; Pu *et al.* 2016). Instead, a correlation with a glacial period recorded in the rest of Cadomia, in NW Africa (Morocco) (Vernhet *et al.* 2012), in Arabia (Vickers-Rich *et al.* 2013) and in Iran (Etemad-Saeed *et al.* 2016) is much more likely and provides more information concerning the timing of this late Ediacaran glacial period. Upper Ediacaran tillites within the Cadomian orogenic belt have been described from the Saxo-Thuringian Zone of the Bohemian Massif and from the Central Iberian Zone of the Iberian Massif (Linnemann *et al.* 2018).

Owing to the lack of datable ash beds, only the oldest age is well constrained for glacigenic sedimentary deposits in Cadomia, provided by maximum depositional ages of *c.* 562 Ma (this study and Linnemann *et al.* 2018). Younger time markers can be determined only based on the intrusions of *c.* 540 Ma aged late Cadomian plutons (Linnemann *et al.* 2014, 2018). The youngest limit of the Upper Ediacaran Glacial Period should be placed much earlier, and a likely correlation with the late Ediacaran glaciations in West Africa and in Arabia constrains the youngest age limit
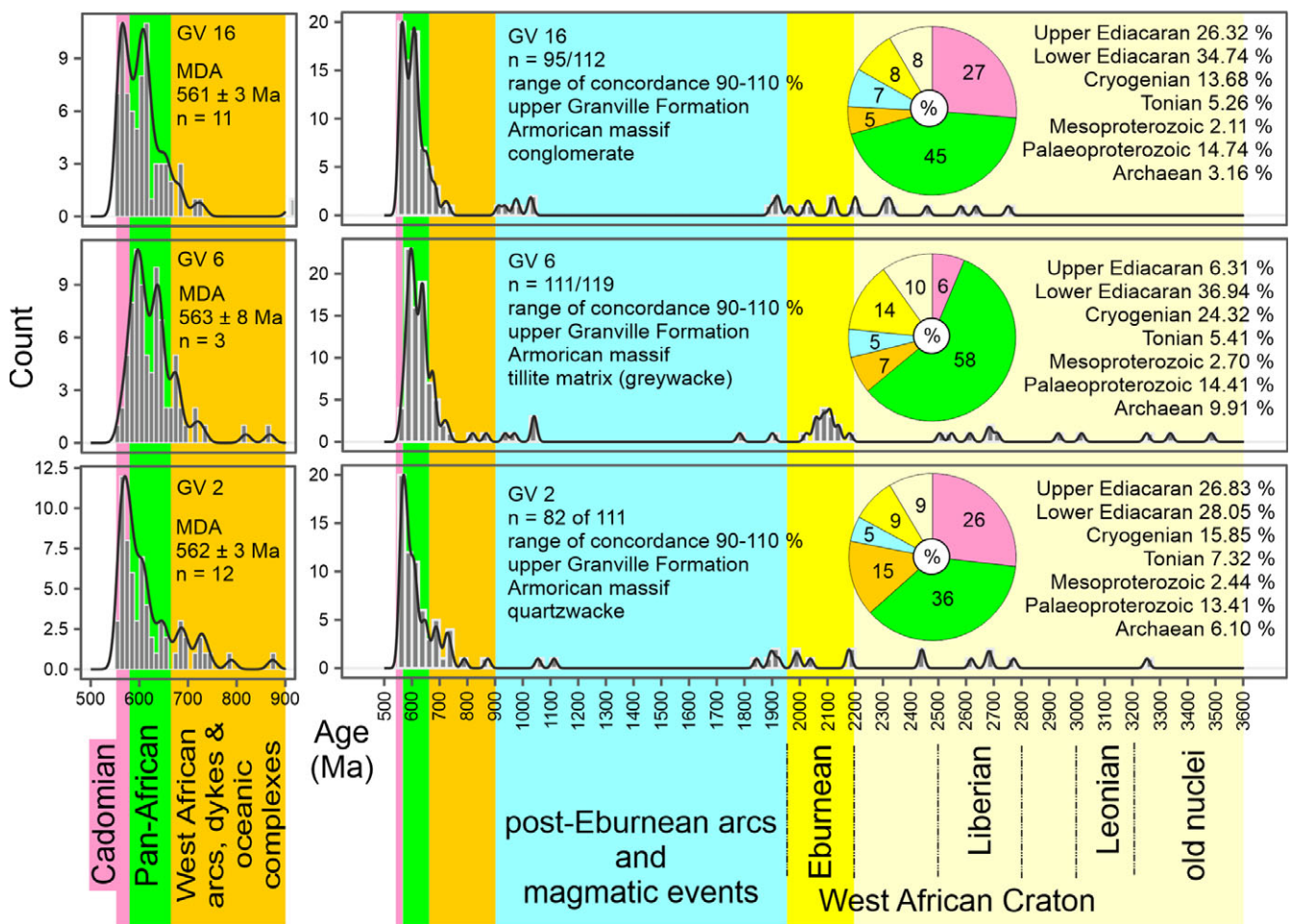
Fig. 10. Age pattern of U–Pb LA-ICP-MS detrital zircon ages of samples GV2, GV6 and GV16 (lower Granville Formation) based on Kernel density estimation plots (Anderson et al. 2018).

(Fig. 11). The Bou Azzer glaciation (West Africa; Verhnet et al. 2012) is recorded associated with rhyolite flows of the Ouarzazate Group, which is constrained by U–Pb zircon ages to a duration of from 569 ± 4 Ma to 567 ± 4 Ma (Karaoui et al. 2015; Errami et al. 2021). The absolute age of the Dhaiqa Formation (Arabia) is reflected by a U–Pb zircon tuff age of 560 ± 4 Ma (Vickers-Rich et al. 2013). A glacial deposit intercalated in the Kahar Formation (Central Elborz Mountains, Iran) yields a maximum depositional age of 560 ± 5 Ma derived from U–Pb detrital zircons (Etemad-Saeed et al. 2016).

We relate the glacial deposits of the Armorican Massif described in this paper with the other occurrences of Cadomia in the Bohemian and Iberian massifs and with the deposits of glaciomarine diamictites in the Anti-Atlas (Bou Azzer) as well as those in Saudi Arabia (Dhaiqa Formation) and the Kahar Formation (Iran). We propose the term 'Upper Ediacaran Glacial Period' for such post-Gaskiers c. 570 Ma to 560 Ma aged glaciomarine deposits (Fig. 11). It should be noted that there are some other rare occurrences of late Ediacaran-aged glacial deposits on Earth. Most are not very well constrained because of their age and/or that their glacigenic nature is currently under discussion (see compilations of Arnaud et al. 2011; Youbi et al. 2020). The two most likely ones are located on the North China craton (Le Heron et al. 2018) and in Tasmania (Calver et al. 2004). Another glacial deposit (Moelv diamictite) with a suggested

Ediacaran age also crops out in Baltica (Bingen et al. 2005), but at present available age data are not sufficient to constrain an age younger than the Gaskiers glaciation. Furthermore, a new U–Pb baddeleyite age for the Ottfjället Dyke Swarm points to a minimum age of 596.3 ± 1.5 Ma for these glacigenic deposits (Kumpulainen et al. 2021).

LA-ICP-MS U–Pb zircon dating is one of the best and most rapid dating methods for detrital zircons. In view of the relatively large errors, the apparent duration of c. 568–561 Ma for the proposed Upper Ediacaran Glacial Period is quite lengthy, noted in Figure 11. Ages obtained using high-precision U–Pb tuff zircon dating for the Marinoan and Gaskiers glacial events constrain such events to a very narrow time corridor (Bowring et al. 2002; Hoffmann et al. 2004; Thompson et al. 2014; Pu et al. 2016; Prave et al. 2016).

Relating the Upper Ediacaran Glacial Period (c. 568–561 Ma) to the δ13C curve shows little overlap with the negative excursion of the Shuram–Wonoka anomaly (Fig. 11; Halverson et al. 2005; Rooney et al. 2020). Halverson et al. (2005) proposed a duration for the Shuram–Wonoka anomaly of between c. 590 Ma and c. 560 Ma. A shorter time interval (581 ± 6 Ma to 567 ± 6 Ma) was later inferred by an age model put forward by Retallack et al. (2014). New age data by Rooney et al. (2020) suggested a more constrained time bracket of between 574.0 ± 4.7 Ma and 567.3 ± 3.0 Ma. That analysis was based on Re–Os geochronology
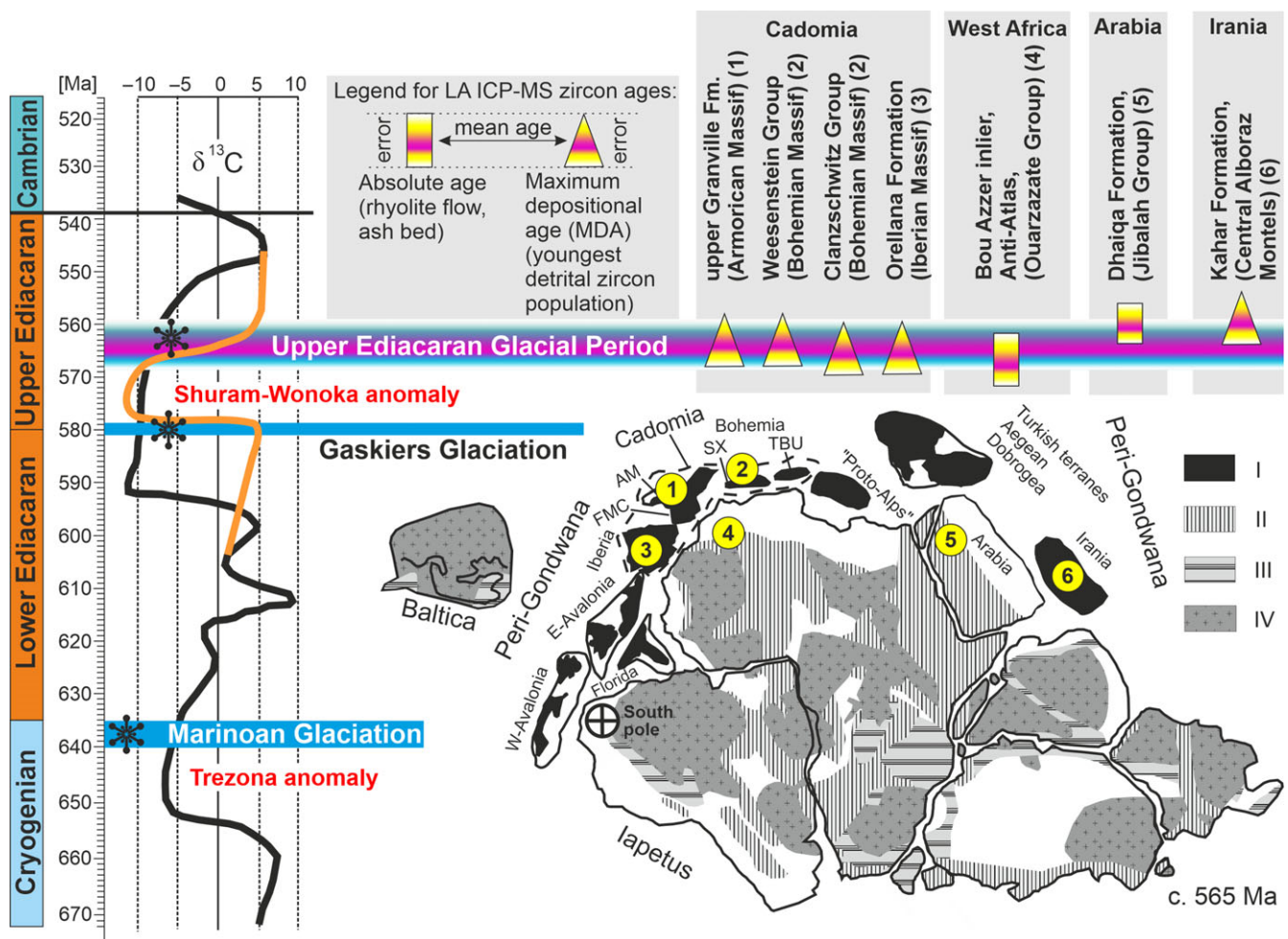
Fig. 11. Timing of the Upper Ediacaran Glacial Period in the Cadomian orogenic belt and related areas and its calibration to the δ^{13}C curve: in black after Halverson *et al.* (2005); in orange modification based on new age constraints for the Shuram–Wonoka anomaly by Rooney *et al.* (2020). Geochronological constraints of the glacial deposits are shown in the upper right of the figure. Bracketed numbers correspond to references. Same numbers mark the palaeogeographical position in the palinspastic map represented in the lower right. Latin numbers: 1 – this study; 2 and 3 – Linnemann *et al.* (2018); 4 – Errami *et al.* (2021); 5 – Vickers-Rich *et al.* (2013); 5 – Etemad–Saeed *et al.* (2016). Roman numbers: I – orogenic belts marginal to Gondwana (peri–Gondwanan Neoproterozoic rocks of the Avalonian and Cadomian orogens and related areas in Turkey, the Aegean, the Dobrogea and Iran); II – Neoproterozoic rocks of the Pan–African orogens in the interior of Gondwana; III – Mesoproterozoic orogenic belts; IV – cratonic areas (Palaeoproterozoic to Archaean) (modified from Linnemann *et al.* 2000).

of organic-rich shales recovered from samples collected in NW Canada and Oman. According to such a result, the timing of the Shuram–Wonoka anomaly has been refined in Figure 11 (orange curve).

All in all, the Gaskiers glacial event does not seem to be a feasible driver of the Shuram–Wonoka event, because it is dated to between *c.* 581 Ma and 579 Ma (Pu *et al.* 2016). Late Ediacaran glaciations also most probably did not contribute to such a negative anomaly. All available age data point to an onset of the Shuram–Wonoka anomaly after the Gaskiers glaciation. Within errors, the final regression of the anomaly overlaps slight with the Upper Ediacaran Glacial Period. Both glacial episodes bracket the anomaly, which means it took place in a warmer climate, and glacial influence is thus ruled out. Ediacaran glaciations do not seem to have impacted the ocean water chemistry.

Our age spectra of U–Pb ages of detrital zircons constrain all glacigenic sediment packages of the upper Granville Formation to the margin of the West African Craton (this study). The same is the case for all other glacial deposits within Cadomia (Linnemann *et al.* 2018). This constrains the palaeoposition of

the origin of the glacigenic tillites to within the Cadomian orogenic belt in southern latitudes at *c.* 60° S (Li *et al.* 2008). Correlatives of the glaciations in Cadomia and West Africa are also present in Arabia and Iran. Such areas had in Ediacaran times palaeopositions at *c.* 30° S (Arabia) and close to the equator (Iran) (Li *et al.* 2008). The spread of late Ediacaran glaciations is patchy and apparently independent of latitude. Most often, these deposits occur on the northern periphery of the Gondwana supercontinent (Fig. 11) and thus are coupled most probably to orogenic processes in peri-Gondwana and related to uplift of higher glaciated mountains in the hinterland of the depositional areas. A modern example of this kind is represented by the more than 2000 km long Patagonian ice sheet, which has been loading the shelf with glaciomarine deposits for the last 35 ka (Davies *et al.* 2020).

Kunst und Tourismus are thanked for permanent financial support of the GeoPlasmaLab (Senckenberg Naturhistorische Sammlungen Dresden). Daniel Le Heron (Universität Wien) and Marjorie Cantine (MIT, Boston) are thanked very much for their fruitful reviews which improved the paper considerably. Further, the authors thank very much Sören Jensen (Universidad de Extremadura, Badajoz) for helpful advice and his editorial work.

References

Abati J, Aghzer AM, Gerdes A and Ennih N (2010) Detrital zircon ages of Neoproterozoic sequences of the Moroccan Anti-Atlas belt. *Precambrian Research* **181**, 115–28.

Abati J, Aghzer AM, Gerdes A and Ennih N (2012) Insights on the crustal evolution of the West African Craton from Hf isotopes in detrital zircons from the Anti-Atlas belt. *Precambrian Research* **212–213**, 263–74.

Andersen T, Kristoffersen M and Elburg MA (2018) Visualizing, interpreting and comparing detrital zircon age and Hf isotope data in basin analysis – a graphical approach. *Basin Research* **30**, 132–47.

Arnaud E, Halverson GP and Shields-Zhou G (eds) (2011) *The Geological Record of Neoproterozoic Glaciations*. Geological Society of London, Memoir no. 36.

Ballèvre M, Bosse V, Ducassou C and Pitra P (2009) Palaeozoic history of the Armorican Massif: models for the tectonic evolution of the suture zones. *Comptes Rendus Geoscience* **341**, 174–201.

Bertrand L (1921) *Les anciennes mers de la France et leur depots*. Paris: Ernest Flammarion.

Bingen B, Griffin WL, Torsvik TH and Saeed A (2005) Timing of Late Neoproterozoic glaciation on Baltica constrained by detrital zircon geochronology in the Hedmark Group, south-east Norway. *Terra Nova* **17**, 250–8.

Bowring SA, Landing E, Myrow P and Ramezani J (2002) Abstract #13045: geochronological constraints on terminal Neoproterozoic events and the rise of metazoans. *Astrobiology* **2**, 457–8.

Bunel H (1835) Observations sur les terrains intermédiaires du département du Calvados. *Mémories de la Société linnéenne de Normandie* **5**, 91–100.

Calver CR, Black LP, Everard JL and Seymour DB (2004) U–Pb zircon age constraints on late Neoproterozoic glaciation in Tasmania. *Geology* **32**, 893–6.

Chantraine J, Auvray B, Brun JP, Chauvel JJ and Rabu D (1994) The Cadomian Orogeny in the Armorican Massif – conclusions. In *Pre-Mesozoic Geology in France* (ed. D Keppie), pp. 126–8. Berlin: Springer.

Davies BJ, Darvill CM, Lovell H, Bendle JM, Dowdeswell JA, Fabel D, García J-L, Geiger A, Glasser NF, Gheorghiu DM, Harrison S, Hein AS, Kaplan MR, Martin JRV, Mendelova M, Palmer A, Pelto M, Rodés Á, Sagredo A, Smedley RK, Smellie JL and Thorndycraft VR (2020) The evolution of the Patagonian Ice Sheet from 35 ka to the recent day. *Earth-Science Reviews* **204**, 103–52.

Davis Jr RA and Fitzgerald DM (2004) *Beaches and Coasts*. Malden. Blackwell Publishing.

D'Lemos RS, Strachan RA and Topley CG (1990) The Cadomian Orogeny in the North Armorican Massif: a brief review. In *The Cadomian Orogeny* (eds RS D'Lemos, RA Strachan and CG Topley), pp. 3–12. Geological Society of London, Special Publication no. 51.

Doré F (1981) Late Precambrian tilloids of Normandy (Armorican Massif). In *Earth's Pre-Pleistocene Glacial Record* (eds MJ Hambrey and WB Harland), pp. 643–6. Cambridge: Cambridge University Press.

Drost K, Gerdes A, Jeffries T, Linnemann U and Storey C (2011) Provenance of Neoproterozoic and early siliciclastic rocks of the Teplá-Barrandian unit (Bohemian Massif): evidence from U–Pb detrital zircon ages. *Gondwana Research* **19**, 213–31.

Dupret L (1984) The Proterozoic of the Northeastern Armorican massif. In *Precambrian in Younger Fold Belts* (ed. V Zoubek), pp. 444–61. New York: Wiley.

Errami E, Linnemann U, Hofmann M, Gärtner A, Zieger J, Gärtner J, Mende K, Kabouri JE, Gasquet D and Ennih N (2021) From Pan-African transpression to Cadomian transtension at the West African margin: new U–Pb zircon ages from the Eastern Saghro Inlier (Anti-Atlas, Morocco). In *Pannotia to Pangaea: Neoproterozoic and Paleozoic Orogenic Cycles in the Circum-Atlantic Region* (eds JB Murphy, RA Strachan and C Quesada), pp. 209–33. Geological Society of London, Special Publication no. 503.

Etemad-Saeed N, Hosseini-Barzi M, Adabi M, Miller NR, Sadeghi A, Houshmandzadeh A and Stockli DF (2016) Evidence for ~560 Ma Ediacaran glaciation in the Kahar Formation, Central Alborz Mountains, northern Iran. *Gondwana Research* **31**, 164–83.

Eyles N (1990) Marine debris flows: late Precambrian "tillites" of the Avalonian-Cadomian orogenic belt. *Palaeogeography, Palaeoclimatology, Palaeoecology* **79**, 73–98.

Faure M, Sommers C, Melleton J, Cocherie A and Lautout O (2010) The Leon Domain (French Massif Armoricain): a westward extension of the Mid-German Crystalline Rise? Structural and geochronological insights. *International Journal of Earth Sciences* **99**, 65–81.

Fernandez-Suarez J, Gutiérrez-Alonso G, Jenner GA and Tubrett MN (2000) New ideas on the Proterozoic-Early Palaeozoic evolution of NW Iberia: insights from U–Pb detrital zircon ages. *Precambrian Research* **102**, 185–206.

Gärtner A, Villeneuve M, Linnemann U, El Archi A and Bellon H (2013) An exotic terrane of Laurussian affinity in the Mauritanides and Souttoufides (Moroccan Sahara). *Gondwana Research* **24**, 687–99.

Graindor MJ (1957) Le Briovérien dans le Nord-Est du Massif Armoricain. In *Mémoires pour servir á l'éxplication de la Carte Géologique détaillée de la France*. Paris: Ministère de l'Industrie et du Commerce, 211 pp.

Graindor MJ (1965) Les tillites ante-cambriennes de Normandie. *Geologische Rundschau* **54**, 61–82.

Halverson GP, Hoffman PF, Schrag DP, Maloof AC and Rice AHN (2005) Toward a Neoproterozoic composite carbon isotope record. *Geological Society of America Bulletin* **117**, 1181–207.

Hoffman PF, Abbot DS, Ashkenazy Y, Benn DI, Brocks JJ, Cohen PA, Cox GM, Creveling JR, Donnadieu Y, Erwin DH, Fairchild IJ, Ferreira D, Goodman JC, Halverson GP, Jansen MF, Le Hir G, Love GD, Macdonald FA, Maloof AC, Partin CA, Ramstein G, Rose BEJ, Rose CV, Sadler PM, Tziperman E, Voigt A and Warren SG (2017) Snowball Earth climate dynamics and Cryogenian geology-geobiology. *Science Advances* **3**, 1–43, e1600983. doi: 10.1126/sciadv.1600983.

Hoffman PF, Kaufman AJ, Halverson GP and Schrag DP (1998) A Neoproterozoic Snowball Earth. *Science* **281**, 1342–6.

Hoffmann KH, Condon DJ, Bowring SA and Crowley JL (2004) U–Pb zircon date from the Neoproterozoic Ghaub Formation Namibia: constraints on Marinoan glaciation. *Geology* **32**, 817–20.

Karaoui B, Breitkreuz C, Mahmoudi A, Youbi N, Hofmann M, Gärtner A and Linnemann U (2015) U–Pb zircon ages from volcanic and sedimentary rocks of the Ediacaran Bas Draâ inlier (Anti-Atlas Morocco): chronostratigraphic and provenance implications. *Precambrian Research* **263**, 43–58.

Kirschvink JL (1992) Late Proterozoic low-latitude global glaciation: the Snowball Earth. In *The Proterozoic Biosphere – A Multidisciplinary Study* (eds JW Schopf and C Klein), pp. 1–52. Cambridge: Cambridge University Press.

Kirschvink JL, Gaidos EJ, Bertani LE, Beukes NJ, Gutzmer J, Maepa LN and Steinberger RE (2000) Paleoproterozoic snowball earth: extreme climatic and geochemical global change and its biological consequences. *Proceedings of the National Academy of Sciences of the United States of America* **97**, 1400–5.

Kumpulainen RA, Hamilton MA, Söderlund U and Nystuen JP (2021) U–Pb baddeleyite age for the Ottfjället Dyke Swarm, central Scandinavian Caledonides: new constraints on Ediacaran opening of the Iapetus Ocean and glaciations on Baltica. *GFF* **143**, 40–54.

Le Heron DP, Vandyk TM, Wu G and Li M (2018) New perspectives on the Luoquan Glaciation (Ediacaran–Cambrian) of North China. *The Depositional Record* **4**, 274–92.

Letsch D, El Houicha M, von Quadt A and Winkler W (2018a) A missing link in the Peri-Gondwanan terrane collage: the Precambrian basement of the Moroccan Meseta and its lower Paleozoic cover. *Canadian Journal of Earth Sciences* **55**, 33–51.

Letsch D, Large SJE, Buechi MW, Winkler M and von Quadt A (2018b) Ediacaran glaciations of the West African Craton – evidence from Morocco. *Precambrian Research* **310**, 17–38.

Li ZX, Bogdanova SV, Collins AS, Davidson A, De Waele B, Ernst RE, Fitzsimons ICW, Fuck RA, Gladkochub DP, Jacobs J, Karlstrom, KE,

Lu S, Natapov LM, Pease V, Pisarevsky SA, Thrane K and Vernikovsky V (2008) Assembly, configuration, and break-up history of Rodinia: a synthesis. *Precambrian Research* **160**, 179–210.

Linnemann U (2007) Ediacaran rocks from the Cadomian basement of the Saxo-Thuringian Zone (NE Bohemian Massif, Germany): age constraints, geotectonic setting and basin development. In *The Rise and Fall of the Ediacaran Biota* (eds P Vickers-Rich and P Komarower), pp. 35–51. Geological Society of London, Special Publication no. 286.

Linnemann U, Gehmlich M, Tichomirowa M, Buschmann B, Nasdala L, Jonas P, Lützner H and Bombach K (2000) From Cadomian subduction to Early Palaeozoic rifting: the evolution of Saxo-Thuringia at the margin of Gondwana in the light of single zircon geochronology and basin development (Central European Variscides, Germany). In *Orogenic Processes: Quantification and Modelling in the Variscan Belt* (eds W Franke, V Haak, O Oncken and D Tanner), pp. 131–53. Geological Society of London, Special Publication no. 179.

Linnemann U, Gerdes A, Hofmann M and Marko L (2014) The Cadomian Orogen: Neoproterozoic to Early Cambrian crustal growth and orogenic zoning along the periphery of the West African Craton—constraints from U–Pb zircon ages and Hf isotopes (Schwarzburg Antiform, Germany). *Precambrian Research* **244**, 236–78.

Linnemann U, McNaughton NJ, Romer RL, Gehmlich M, Drost K and Tonk C (2004) West African provenance for Saxo-Thuringia (Bohemian Massif): did Armorica ever leave pre-Pangean Gondwana? – U/Pb-SHRIMP zircon evidence and the Nd-isotopic record. *International Journal of Earth Sciences* **93**, 683–705.

Linnemann U, Ouzegane K, Drareni A, Hofmann M, Becker S, Gärtner A and Sagawe A (2011) Sands of West Gondwana: an archive of secular magmatism and plate interactions – a case study from the Cambro-Ordovician section of the Tassili Ouan Ahaggar (Algerian Sahara) using U–Pb-LA-ICP-MS detrital zircon ages. *Lithos* **123**, 188–203.

Linnemann U, Ovtcharova M, Schaltegger U, Gärtner A, Hautmann M, Geyer G, Vickers-Rich G, Rich T, Plessen B, Hofmann M, Zieger J, Krause R, Kriesfeld L and Smith J (2019) New high-resolution age data from the Ediacaran–Cambrian boundary indicate rapid, ecologically driven onset of the Cambrian explosion. *Terra Nova* **31**, 49–58.

Linnemann U, Pidal AP, Hofmann M, Drost K, Quesada C, Gerdes A, Marko L, Gärtner A, Zieger J, Ulrich J, Krause R, Vickers-Rich P and Horak J (2018) A ~565 Ma old glaciation in the Ediacaran of peri-Gondwanan West Africa. *International Journal of Earth Sciences* **107**, 885–911.

Ludwig KR (2008) *User's Manual for Isoplot 3.00: A Geochronological Toolkit for Microsoft Excel.* Berkeley Geochronology Center, Special Publication no. 4, 76 pp.

Murphy JB and Nance RD (1991) Supercontinent model for the contrasting character of Late Proterozoic orogenic belts. *Geology* **19**, 469–72.

Nance RD, Gutiérrez-Alonso G, Keppie JD, Linnemann U, Murphy JB, Quesada C, Strachan RA and Woodcock NH (2010) Evolution of the Rheic Ocean. *Gondwana Research* **17**, 194–222.

Narbonne GM and Gehling JG (2003) Life after snowball: the oldest complex Ediacaran fossils. *Geology* **31**, 27–30.

Narbonne GM, Laflamme M, Trusler PW, Dalrymple RW and Greentree C (2014) Deep-water Ediacaran fossils from northwestern Canada: taphonomy, ecology, and evolution. *Journal of Paleontology* **86**, 207–23.

Potrel A, Peucat JJ and Fanning CM (1998) Archean crustal evolution of the West African Craton: example of the Amsaga Area (Reguibat Rise) U–Pb and Sm–Nd evidence for crustal growth and recycling. *Precambrian Research* **90**, 107–17.

Prave AR, Condon DJ, Hoffmann KH, Tapster S and Fallick AE (2016) Duration and nature of the end-Cryogenian (Marinoan) glaciation. *Geology* **44**, 631–4.

Pu JP, Bowring SA, Ramezani J, Myrow P, Raub TD, Landing, E, Mills A, Hodgin E and Macdonald FA (2016) Dodging snowballs: geochronology of the Gaskiers glaciation and the first appearance of the Ediacaran biota. *Geology* **44**, 955–8.

Ravier E, Buoncristiani J-F, Guiraud M, Menzies J, Clerc S, Goupy B and Portier E (2014) Porewater pressure control on subglacial soft sediment remobilization and tunnel valley formation: a case study from the Alnif tunnel valley (Morocco). *Sedimentary Geology* **304**, 71–95.

Retallack GJ, Marconato A, Osterhout JT, Watts KE and Bindeman IN (2014) Revised Wonoka isotopic anomaly in South Australia and Late Ediacaran mass extinction. *Journal of the Geological Society, London* **171**, 709–22.

Rooney AD, Cantine MD, Bergmann KD, Gómez-Pérez I, Al Baloushi B, Boag TH, Busch JF, Sperling EA and Strauss JV (2020) Calibrating the coevolution of Ediacaran life and environment. *Proceedings of the National Academy of Sciences of the United States of America* **117**, 16824–30.

Schermerhorn LJG (1974) Late Precambrian mixtites: glacial and/or nonglacial? *American Journal of Science* **274**, 673–824.

Skolasińska K, Rachlewicz G and Szczuciński W (2016) Micromorphology of modern tills in southwestern Spitsbergen – insights into depositional and post-depositional processes. *Polish Polar Research* **37**, 435–56.

Thompson MD, Ramezani J and Crowley JL (2014) U–Pb zircon geochronology of Roxbury conglomerate, Boston Basin, Massachusetts: tectono-stratigraphic implications for Avalonia in and beyond SE New England. *American Journal of Science* **314**, 1009–40.

Vernhet E, Youbi N, Chellai EH, Villeneuve M and El Archi A (2012) The Bou-Azzer glaciation: evidence for an Ediacaran glaciation on the West African Craton (Anti-Atlas, Morocco). *Precambrian Research* **196–197**, 106–12.

Vickers-Rich P, Kozdroj W, Kattan FH, Leonov M, Ivantsov A, Johnson PR, Linnemann U, Hofmann M, Al Garni SM, Al Qubsani A, Shamari A, Al Barakati A, Al Kaff MH, Ziolkowska-Kozdroj M, Rich T, Trusler P and Rich B (2013) *Reconnaissance for an Ediacaran Fauna, Kingdom of Saudi Arabia.* Technical Report SGS-TR-2010-8. Jeddah: Saudi Geological Survey, 42 pp.

Wegmann CE (1951) Subkambrische Tillite in der herzynischen Faltungszone. *Geologische Rundschau* **39**, 221–34.

Wegmann CE, Dangeard L and Graindor JM (1950) Sur quelques caractères remarquables de la formation précambrienne connue sours le nom de poudingue de Granville. *Comptes Rendus de l'Académie des Sciences* **230**, 979–80.

Xiao SH and Narbonne GM (2020) Ediacaran Period (Chapter 18). In *Geologic Time Scale 2020* (eds FM Gradstein, JG Ogg, MD Schmitz and Ogg GM), pp. 521–61. Amsterdam: Elsevier.

Xiao S, Narbonne GM, Zhou C, Laflamme M, Grazhdankin DV, Moczydlowska-Vidal M and Cui H (2016) Towards an Ediacaran time scale: problems, protocols, and prospects. *Episodes* **39**, 540–55.

Youbi N, Ernst RE, Söderlund U, Boumehdi MA, Ait Lahna A, Tassinari CCC, El Moume W and Bensalah MK (2020) The Central Iapetus magmatic province: an updated review and link with the ca. 580 Ma Gaskiers glaciation. In *Mass Extinctions, Volcanism, and Impacts: New Developments* (eds T Adatte, DPG Bond and G Keller), pp. 35–66. Geological Society of America Special Papers 544. doi: 10.1130/2020.2544(02).